Editors' Suggestion

Observation of Acoustically Induced Transparency for γ-Ray Photons

Y. V. Radeonychev,[1,2,5,*] I. R. Khairulin,[1,5] F. G. Vagizov,[3,4,2] Marlan Scully,[4] and Olga Kocharovskaya[4]
[1]Institute of Applied Physics of the Russian Academy of Sciences, 46 Ulyanov Street, Nizhny Novgorod 603950, Russia
[2]Kazan E.K. Zavoisky Physical-Technical Institute of the Kazan Scientific Center of the Russian Academy of Sciences, 10/7 Sibirsky tract, Kazan 420029, Russia
[3]Kazan Federal University, 18 Kremlyovskaya Street, Kazan 420008, Russia
[4]Department of Physics and Astronomy and Institute for Quantum Studies and Engineering, Texas A&M University, College Station, Texas 77843-4242, USA
[5]N. I. Lobachevsky State University of Nizhny Novgorod, 23 Gagarin Avenue, Nizhny Novgorod 603950, Russia

(Received 17 October 2019; accepted 2 April 2020; published 24 April 2020)

We report an observation of a 148-fold suppression of resonant absorption of 14.4 keV photons from $\exp(-5.2)$ to $\exp(-0.2)$ with preservation of their spectral and temporal characteristics in an ensemble of the resonant two-level ^{57}Fe nuclei at room temperature. The transparency was induced via collective acoustic oscillations of nuclei. The proposed technique allows extending the concept of induced optical transparency to a hard x-ray or γ-ray range and paves the way for acoustically controllable interface between x-ray or γ-ray photons and nuclear ensembles, advancing the field of x-ray or γ-ray quantum optics.

DOI: 10.1103/PhysRevLett.124.163602

The induced transparency of opaque medium for resonant electromagnetic radiation is a powerful tool for manipulating the field-matter interaction. This phenomenon was observed in different physical systems in a wide spectral range of electromagnetic waves from microwaves to γ rays [1–13]. Recently, induced transparency was also demonstrated for acoustic waves [14,15]. Self-induced transparency [1], transparency via Autler-Townes splitting (ATS) [2–4], and electromagnetically induced transparency (EIT) [5,6] including their analogs in various quantum and classical systems [6–12], are just several examples of numerous techniques for suppression of resonant absorption. Numerous applications of induced optical transparency for realization of optical switchers, delay lines, quantum memories, quantum gates, etc., stimulate the development of similar techniques in the hard x-ray or soft γ-ray domain.

Narrow-bandwidth heralded high-energy (10–100 keV) photons can be produced by the synchrotron Mössbauer sources (SMS) [16,17] as well as by the radioactive sources with the cascade scheme of decay [11,13]. They can be more easily detected than optical photons and well focused [18], as well as penetrate through many optically opaque materials. The corresponding resonant recoilless (Mössbauer) nuclear transitions have a few orders of magnitude narrower linewidths at room temperature than transitions of bound electrons in atoms. Together with the high density of the nuclei in a solid, this allows for a large resonant optical depth with a small physical length of the absorber [13,19]. These features are promising for realization of very compact and efficient interfaces between single hard x-ray or soft γ-ray photons and nuclear ensembles [20]. However, the common tools for controlling quantum interfaces, such as intense spectrally narrow coherent sources and high-finesse cavities are still unavailable in the hard x-ray or γ-ray range, preventing from a direct realization of the basic optical transparency techniques such as EIT and ATS transparency, for high-energy photons.

Several different techniques to control resonant interaction between hard x-ray or γ-ray photons and nuclear ensembles were developed. They are based on variation of the hyperfine or external magnetic field [11,21,22], mechanical displacement (periodic or nonperiodic) of an absorber or source with respect to each other including acoustic vibration [13,19,23–32], and placing nuclei into spatial sandwichlike nanostructures forming the planar waveguides [12]. The 25% reduction in absorption of 14.4 keV photons was observed via anticrossing of the upper energy sublevels of ^{57}Fe nuclei in a crystal of $FeCO_3$ taking place at 30 K [11]. The achieved magnitude of the absorption reduction (25%) is limited by the intrinsic physical properties of the crystal. The 4.5-fold suppression of 14.4 keV collective coherent emission in the given direction from two ^{57}Fe layers imbedded into a specifically designed planar waveguide was reported in [12]. The 15-fold emission suppression is expected to be achieved in the ideal case of the single-line ^{57}Fe absorber [12].

A common technique for controlling the resonant absorption of x rays or γ rays (which is the basis of Mössbauer spectroscopy) is to use the Doppler shift in the frequency of incident radiation with respect to the spectral line of the absorber, caused by the relative motion of the source and absorber. This technique is very efficient due to both the short radiation wavelength and narrow linewidths

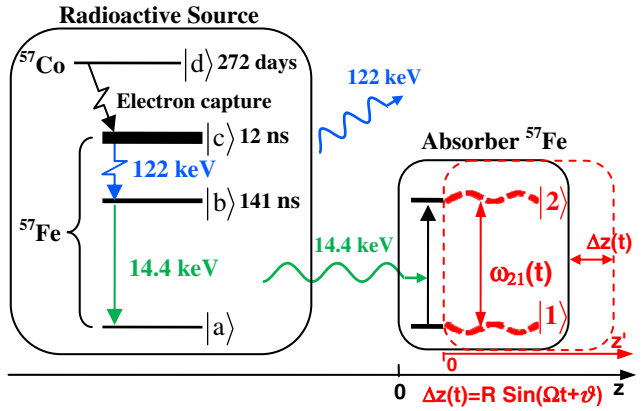

FIG. 1. Energy scheme of the radioactive source of 14.4 keV photons and the vibrating absorber used in the experiment. The ^{57}Co nuclei (left side) in the state $|d\rangle$ decay to ^{57}Fe nuclei in the excited state $|c\rangle$ (with a half-life of $T_{1/2} \approx 272$ day), followed by cascade decay: $|c\rangle \to |b\rangle$ (with decay time $T \approx 12$ ns) and $|b\rangle \to |a\rangle$ (with decay time $T_S \approx 141$ ns) with emission of 122 and 14.4 keV photons (shown by blue and green lines), respectively. Depolarized recoilless 14.4 keV photons ($\lambda \approx 0.86$ Å) resonantly interact with transition $|1\rangle \to |2\rangle$ of ^{57}Fe nuclei when propagating through the single-line ^{57}Fe absorber (right side). They are resonantly absorbed in motionless absorber (black lines). Harmonic vibration of the absorber as a whole (pistonlike vibration) with circular frequency Ω, amplitude R, and initial phase ϑ along the photon propagation direction (marked in red) leads to periodic temporary variation in $|1\rangle \to |2\rangle$ transition frequency $\omega_{21}(t)$ (dashed red curves) due to the Doppler effect. It modifies the interaction of the photon with absorber and can result in AIT (see Fig. 2 and text). The axis z labels the laboratory reference frame, red axis z' labels the reference frame of the vibrating absorber, and $\Delta z = z - z'$.

of nuclear recoilless resonances. For example, motion of the ^{57}Fe absorber at a constant velocity of 0.17 mm/s along the photon propagation direction shifts the position of its 1.13 MHz-wide spectral line, centered at wavelength of 0.86 Å, by 2 MHz. In the case of acoustic vibration of the absorber, the resonant transition frequency of the nuclei is periodically shifted relative to the photon frequency (Fig. 1, right side), leading to appearance of the equidistant sidebands in the absorption spectrum, symmetrically located near the parent spectral line and separated by the vibration frequency [23,28,30]. In the case of synchronous vibrations of nuclei with the same amplitude (pistonlike absorber vibration), an incident quasimonochromatic radiation is efficiently transformed into a spectral comb at the frequencies of sidebands [24]. This is accompanied by a significant increase in resonant transmission up to 70% in Refs. [13,26] and over 80% in Ref. [24]. If spectral phases of the sidebands are synchronized, such a spectral comb can correspond to a regular sequence of short near-bandwidth limited γ-ray pulses experimentally demonstrated in Refs. [13,26]. A similar efficient transformation of quasimonochromatic vacuum ultraviolet and extreme

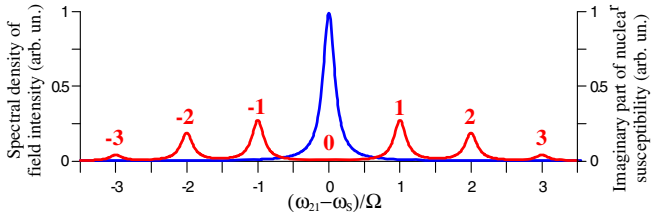

FIG. 2. Spectrum of an incident photon and the absorption spectral profile of the nuclear transition in the case of the harmonically vibrating absorber under AIT conditions. In the laboratory reference frame, the blue curve is the Lorentz spectral profile of the incident field with half-linewidth γ_S and the red curve is the spectral line of the absorber's frequency-modulated transition $|1\rangle \to |2\rangle$ (indicated by red dashed curves in Fig. 1) with half Lorentzian-linewidth $\gamma_{21} = \gamma_S$, harmonically vibrating with circular frequency $\Omega/\gamma_{21} = 10$ and amplitude $R = R_1$. Equivalently, in the vibrating reference frame the blue curve is the spectral line of the same absorber and the red curve is the spectral profile of the same field, "seen" by oscillating nuclei [see Eqs. (S7),(S8),(S22),(S27) in the Supplemental Material [36]]. Here ω_{21} and ω_S are the frequencies of the nuclear transitions of the absorber and the photon source, respectively.

ultraviolet radiation into attosecond pulses under strong suppression of the resonant absorption can be realized in atomic gas or plasma, when the resonant transition frequency of atoms or ions is periodically modulated by a strong laser field via Stark effect [25,33–35].

However, the possibility of complete transmission of hard x-ray or γ-ray photon through an optically deep resonant nuclear absorber without any alterations of its spectral profile and the temporal waveform has never been demonstrated so far. In this work, we show that the proper acoustical vibration of an absorbing medium can provide such full transparency completely eliminating the resonant interaction of γ-ray photons with an optically deep nuclear absorber. We determine the conditions for such acoustically induced transparency (AIT) and demonstrate this technique in a proof-of-principle experiment with the 14.4-keV recoilless individual photons propagating through the ^{57}Fe resonant nuclear absorber (see the energy scheme in Fig. 1). We show that the effect of AIT is robust, i.e., a sufficiently high degree of transparency may be achieved even in the case of a substantial deviation from the AIT conditions.

The physical origin of AIT is especially evident in the reference frame of the vibrating absorber (Fig. 2). In the vibrating reference frame where $z' = z - R\sin(\Omega t + \vartheta)$ (see definitions in Figs. 1, 2), each Fourier constituent, $\bar{E}_S(\omega_S)e^{-i\omega_S t + ik_S z}$ [where $\bar{E}_S(\omega_S)$ is the spectral amplitude of the field at frequency ω_S, $k_S = \omega_S/c$ is the wave number, and c is the speed of light in vacuum], of the incident field acquires a phase modulation due to the Doppler effect, $e^{-i\omega_S t + ik_S z' + ik_S R\sin(\Omega t+\vartheta)}$. According to the Jacobi-Anger formula, $\exp\{\pm ip\sin\phi\} = \sum_{n=-\infty}^{\infty} J_n(p)\exp(\pm in\phi)$ [where $J_n(p)$ is the nth Bessel function of the first kind], it is

"seen" by nuclei as a frequency comb. As a result, the single Lorentz spectral line of the photon source in the laboratory reference frame (Fig. 2, blue curve) corresponds to a set of spectral lines in the vibrating reference frame (Fig. 2, red line; also see the Supplemental Material [36]) [13,26,31,32]. Amplitudes of the spectral lines are proportional to Bessel functions [13,26,31,32], $J_n(2\pi R/\lambda)$, where n is the number of the spectral line and $\lambda = 2\pi/k_S$ is the photon wavelength. If the vibration amplitude R takes the value

$$R = R_i, \quad \text{where } R_1 \approx 0.38\lambda, R_2 \approx 0.88\lambda, R_3 \approx 1.37\lambda, \ldots, \quad (1)$$

then $J_0(2\pi R_i/\lambda) \approx 0$, i.e., the resonant (zero) spectral line vanishes and all the photon energy is spread among the sidebands (Fig. 2). In the ideal case of the monochromatic weak field and infinitely narrow spectral line of the absorber, the spectral sidebands are out of resonance and propagate through the medium without interaction with nuclei. In other words, the absorber is completely transparent for radiation.

Since the spectral lines of both the source and absorber are broadened, the sidebands of the field in the vibrating reference frame overlap with the absorber spectral line (Fig. 2). This results in spectrally selective absorption and dispersion of the propagating field, which cannot be neglected for the optically deep absorber. Hence, in order to achieve transparency for radiation with half-linewidth γ_S in absorber with half-linewidth γ_{21} and optical depth $T_M > 1$ (corresponding to $e^{-T_M} < 0.37$), vibrating with circular frequency Ω, two additional conditions should be met:

$$\gamma_S/\Omega \ll 1, \quad (2a)$$

$$T_M\gamma_{21}/(2\Omega) \ll 1. \quad (2b)$$

If condition (1) is fulfilled, then the resonant spectral component of the incident field vanishes (Fig. 2), whereas conditions (2) mean that the sidebands are located so far from the absorber spectral line that both the resonant absorption and dispersion of the absorber do not affect the field over the entire propagation length. Hence, neither spectral nor temporal characteristics of the incident field are changed, which is equivalent to complete transparency of the resonant medium.

It is worth noting that conditions (1), (2) do not imply the determined initial phase of vibration. This means that AIT can be implemented not only by absorber vibration but also by an acoustic wave or even by random oscillations of nuclei with the same amplitude and frequency (also see Supplemental Material [36]).

Equivalently, in the laboratory reference frame, the spectral line of the absorber under AIT-conditions (1), (2) is "seen" by the photon as a spectral comb containing only the sidebands but not the resonant component (Fig. 2), resulting in negligible interaction of photon with nuclei [see equations (S14)–(S15),(S19),(S23)–(S28) in the Supplemental Material [36]].

The spectral window of AIT in Fig. 2 appears due to a splitting of the absorber spectral line into sidebands having the linewidths of the parent line. This is similar to the transparency induced by the ATS [2–4] (see also Supplemental Material [36]). In both cases, the minimum width of the transparency window is determined by the resonant transition linewidth. In the considered case of the ^{57}Fe nuclei at room temperature, it is about 1 MHz that is 5 orders of magnitude narrower than ATS transparency window, which could be achieved at optical transitions in solids at room temperature and is comparable to the EIT transparency window in color centers of diamond at liquid-helium temperatures [37].

It is worth mentioning that in the case when the carrier frequency of the incident photon is far detuned from the spectral line of the motionless absorber (so that the photon is not absorbed), the absorber vibration with a frequency equal to the detuning (or with a subharmonic of the detuning) would tune one of the sidebands of the nuclear spectral line into resonance with the photon frequency, resulting in acoustically induced absorption. Such absorption would be accompanied by both spectral and temporal distortions of the photon during its propagation through the absorber [25].

Experimental demonstration of AIT was implemented with the radioactive source ^{57}Co:Rh and stainless steel foil as the absorber with the optical depth (Mössbauer thickness) $T_M \approx 5.2$, vibrating as a whole with frequency $\Omega/(2\pi) \approx 9.87$ MHz (Figs. 3–5). The half linewidths of the source and absorber were $\gamma_S/(2\pi) \approx 0.68$ and $\gamma_{21}/(2\pi) \approx 0.85$ MHz (see Supplemental Material [36]). Thus, the sidebands of the nuclear response (red curve in Fig. 2) were well resolved, $\Omega/\gamma_{21} \approx 11.6$. However, conditions (2) were not perfectly satisfied since $\gamma_S/\Omega \approx 0.07$ and $T_M\gamma_{21}/(2\Omega) \approx 0.2$. In order to meet condition (1), the vibration amplitude was adjusted to value $R_1 \approx 0.33$ Å and monitored via the Mössbauer transmission spectrum of the vibrating absorber [Figs. 3(a), 3(b)].

The transmission spectrum in Fig. 3(b) qualitatively corresponds to the spectral line of the vibrating absorber in (Fig. 2 red curve) with two major differences. The first one is the larger broadening of the measured spectral components caused by a number of factors (see Supplemental Material [36]). The second one is the non-vanishing resonant (central) component (unlike the red curve in Fig. 2). This is due to slightly different vibration amplitudes of different parts of the foil within the beam spot (see Supplemental Material [36]). Hence condition (1) was not perfectly satisfied too. Nevertheless, a substantial suppression of the resonant spectral component compared to the sidebands shows that the most probable vibration amplitude was 0.33 Å. Therefore, high transparency of the absorber for 14.4 keV photons could be expected. This was

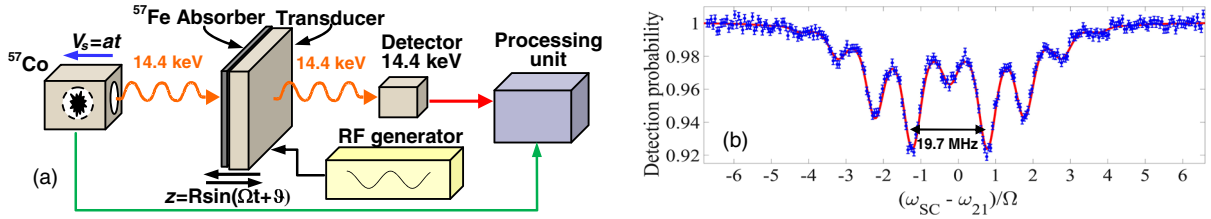

FIG. 3. Absorber transmission spectrum. (a) Generic scheme of the experimental setup. The ^{57}Co:Rh source is moved with constant acceleration along the photon propagation direction. The absorber is 25 μm-thickness stainless steel foil of Fe:Cr:Ni; 70:19:11 wt% with natural abundance (~2%) of ^{57}Fe corresponding to optical depth $T_M \approx 5.2$. The foil is glued on the sinusoidally vibrated polyvinylidene fluoride piezoelectric transducer. (b) Mössbauer transmission spectrum, i.e., the dependence of probability of detecting the transmitted 14.4 keV photons per unit time on the detuning between the variable central frequency of the source spectral line, ω_{SC}, and the fixed central frequency of the absorber spectral line, ω_{21}, normalized by the transmittance far from resonance. Blue dots are the measured values with error bars estimated from counting statistics as $\sqrt{N(\omega)}/N_m$, where $N(\omega)$ is the number of counts for frequency ω and $N_m = N(\omega = \pm\infty)$ is the maximum of function $N(\omega)$. Red fitting curve is plotted according to formulas (S35)–(S36) in the Supplemental Material [36], which take into account the experimental conditions such as the difference in vibration amplitudes of the foil within the beam spot, the spectral line broadening of the source and absorber, as well as the background illumination of the detector.

verified via measuring the spectrum and waveform of the transmitted photons.

The measured spectrum of the resonant 14.4 keV single-photon wave packet behind the vibrating absorber in comparison with the cases of in-resonance and far-off-resonance motionless absorber and the corresponding experimental setup are shown in Fig. 4. The striking difference between red and green curves in Fig. 4(b) proves that despite the nonperfect implementation of the AIT conditions (1), (2), the resonant absorption is greatly reduced in the vibrating absorber as compared to the absorber at rest. Achieved efficiency of AIT evaluated as the ratio between the amplitudes of solid red and dotted black curves, is 82% corresponding to 26 times reduction of the effective optical depth from 5.2 of the motionless absorber to 0.2 in the implemented case of AIT. Similar to the spectral line of the incident photons [black dotted curve in Fig. 4(b)], red line in Fig. 4(b), has nearly Lorentz profile except that barely noticeable sidebands appeared due to incomplete fulfillment of AIT conditions (1), (2).

The waveform of the transmitted photons (the time dependence of the photon detection probability proportional to intensity of the single-photon wave packet) was measured via the time-delayed coincidence technique of the Mössbauer time-domain spectroscopy [Fig. 5(a)]. In the case of the motionless absorber, the output waveforms of the in-resonance photons and far-off-resonance photons are dramatically different [solid green and dotted black curves, respectively, in Fig. 5(b)]. In the case of the vibrating absorber under the implemented AIT, they almost coincide [solid red and dotted black curves, respectively, in Fig. 5 (b)], showing that the waveform of the incident photon is preserved. The analysis of both spectral and temporal characteristics of the transmitted photons (Figs. 4, 5) shows also that AIT is a robust effect, whose appearance does not require a strict compliance with the AIT conditions (1), (2).

The main factor limiting the efficiency of AIT is inhomogeneity of the vibration amplitude of the absorber across the beam of γ radiation, which leads to violation of condition (1). This inhomogeneity can be reduced via

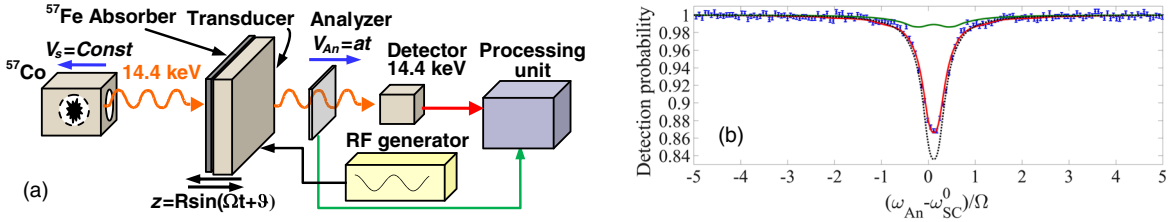

FIG. 4. Transmitted photon spectrum. (a) Generic scheme of the experimental setup. Unlike Fig. 3, the source is moved at a constant velocity v_S compensating the isomer shift, so that its resonant frequency ω^0_{SC} coincides with the absorber resonant frequency. Spectrum of the transmitted radiation is measured by analyzer which is stainless steel foil with the same characteristics as characteristics of the absorber. Analyzer is moved with constant acceleration such that the moment of detection of the 14.4 keV photon defines the central frequency of the analyzer spectral line, ω_{An} (see Supplemental Material [36]). (b) Probability of detection of the 14.4 keV photon per unit time versus the detuning between variable resonance frequency of analyzer, ω_{An}, and resonance frequency of the source, ω^0_{SC}. Blue dots with error bars are the measured values. Red line is the theoretical fitting compared to the case of the motionless absorber tuned to resonance (solid green line) or far from resonance (dotted black line). Theoretical curves are plotted according to formula (S37) in the Supplemental Material [36].

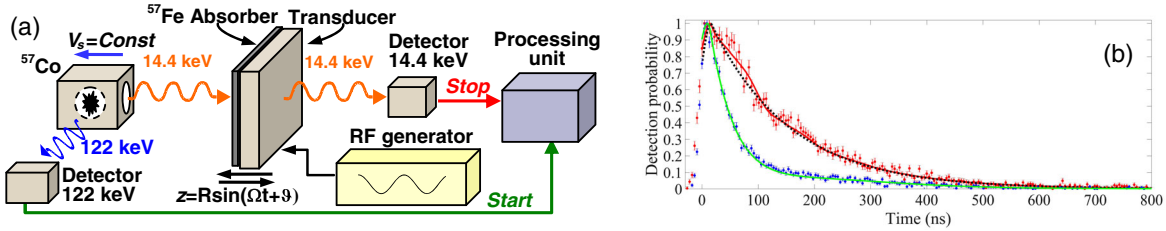

FIG. 5. Transmitted photon waveforms. (a) Generic scheme of the time-delayed coincidence counting sequential 122 and 14.4 keV photons. The interval between "Start" and "Stop" signals measured many times gives the coincidence count rate as a function of delay, proportional to the time dependence of photon detection probability or, equivalently, to the single-photon waveform. The source is moved with constant velocity v_S to match resonant frequencies of the source and absorber. (b) The measured waveforms of 14.4-keV photons transmitted through the motionless resonant absorber (blue dots with error bars) and through the vibrating absorber (red dots with error bars) in comparison with the waveform of the photon passed through the far-off-resonant motionless absorber (black dotted line). Red, green, and black curves are plotted according to formula (S38) in the Supplemental Material [36]. The waveforms in red, green, and black correspond to spectral contours of the same color in Fig. 4(b).

decrease of the illuminated part of the foil (i) using the lead mask in front of the absorber with a smaller hole (at the cost of a longer acquisition time) in the case of the radioactive source, or (ii) using a well-focused spectrally bright SMS [16,17]. Additional opportunities in the implementation and applications of AIT with SMS include the possibility to synchronize the synchrotron radiation pulses with the absorber vibration, and to control the bandwidth, waveform, and polarization of x-ray photons [38,39].

AIT can be used for switching and chopping the transmitted photons. The switching time can be as fast as a fraction of a nanosecond for diamond piezoelectric transducers [40] and up to 20 ps for polyvinylidene fluoride transducers [41]. Other potential applications of AIT include a reduction of self-absorption in high-activity radioactive sources with large optical depth, as well as Mössbauer spectroscopy of optically deep targets.

The AIT spectral window is accompanied by relatively steep absorber dispersion leading to the slowing down of the group velocity of the γ-ray single-photon wave packet. Narrow width of the Mössbauer spectral lines, short photon wavelengths, and the large density of nuclei in a solid absorber allow for significant reducing of the group velocity of γ rays in the case of AIT. In the present experiment, the 19.7 MHz-wide spectral window of AIT [Fig. 3(b)] corresponds to a 14.4 keV-photon group velocity of 5.6×10^3 m/s (see Supplemental Material [36]), which is comparable to the values achieved by other techniques [11,42,43]. Optimization of this experiment via an appropriate reduction in the absorber vibration frequency and its enrichment with ^{57}Fe would allow slowing down 14.4 keV photons below 20 m/s at room temperature [44,45]. Finally, the proposed AIT, similar to optical EIT, can become the basis for realization of acoustically controllable interfaces between γ-ray photons and nuclear ensembles.

We are grateful to T. R. Akhmedzhanov for assistance in conducting experimental measurements and to Yury Shvyd'ko for stimulating discussions. We acknowledge support by the Russian Foundation for Basic Research (RFBR, Grants No. 18-32-00774 and No. 19-02-00852), as well as support by the National Science Foundation (NSF, Grants No. PHY-150-64-67 and No. PHY -182-09-30), Air Force Office of Scientific Research (Grant No. FA9550-18-1-0141), Office of Naval Research (Grant No. N00014-20-1-2184), and by the Robert A. Welch Foundation (Grant No. A-1261). M. O. S. also appreciates support by the King Abdulaziz City for Science and Technology (KACST) program. The numerical studies were supported by the Ministry of Science and Higher Education of the Russian Federation under Contract No. 14.W03.31.0032. I. R. Kh. acknowledges support by the Foundation for the Advancement of Theoretical Physics and Mathematics "BASIS". Y. V. R. acknowledges financial support of his analytical studies from the Government of the Russian Federation (Mega-Grant No. 14.W03.31.0028).

*Corresponding author.
radion@appl.sci-nnov.ru

[1] S. L. McCall and E. L. Hahn, Self-Induced Transparency by Pulsed Coherent Light, Phys. Rev. Lett. **18**, 908 (1967).
[2] S. H. Autler and C. H. Townes, Stark effect in rapidly varying fields, Phys. Rev. **100**, 703 (1955).
[3] O. Kocharovskaya and Y. V. Radeonychev, Spontaneous emission from the ground atomic state due to its crossing with the dynamic Stark level, Found. Phys. **28**, 561 (1998).
[4] E. Saglamyurek, T. Hrushevskyi, A. Rastogi, K. Heshami, and L. J. LeBlanc, Coherent storage and manipulation of broadband photons via dynamically controlled Autler–Townes splitting, Nat. Photonics **12**, 774 (2018).
[5] O. Kocharovskaya and Ya. I. Khanin, Population trapping and coherent bleaching of a three-level medium by a periodic train of ultrashort pulses, Sov. Phys. JETP **63**, 945 (1986), http://www.jetp.ac.ru/cgi-bin/e/index/e/63/5/p945?a=list.
[6] K. J. Boller, A. İmamoğlu, and S. E. Harris, Observation of Electromagnetically Induced Transparency, Phys. Rev. Lett. **66**, 2593 (1991).

[7] S. Weis, R. Rivière, S. Delèglise, E. Gavartin, O. Arcizet, A. Schliesser, and T. J. Kippenberg, Optomechanically induced transparency, Science **330**, 1520 (2010).

[8] S. Zhang, D. Genov, Y. Wang, M. Liu, and X. Zang, Plasmon-Induced Transparency in Metamaterials, Phys. Rev. Lett. **101**, 047401 (2008).

[9] A. G. Litvak and M. D. Tokman, Electromagnetically Induced Transparency in Ensembles of Classical Oscillators, Phys. Rev. Lett. **88**, 095003 (2002).

[10] K. Totsuka, N. Kobayashi, and M. Tomita, Slow Light in Coupled-Resonator-Induced Transparency, Phys. Rev. Lett. **98**, 213904 (2007).

[11] R. Coussement, Y. Rostovtsev, J. Odeurs, G. Neyens, H. Muramatsu, S. Gheysen, R. Callens, K. Vyvey, G. Kozyreff, P. Mandel, R. Shakhmuratov, and O. Kocharovskaya, Controlling Absorption of Gamma Radiation via Nuclear Level Anticrossing, Phys. Rev. Lett. **89**, 107601 (2002).

[12] R. Röhlsberger, H.-C. Wille, K. Schlage, and B. Sahoo, Electromagnetically induced transparency with resonant nuclei in a cavity, Nature (London) **482**, 199 (2012).

[13] F. Vagizov, V. Antonov, Y. V. Radeonychev, R. N. Shakhmuratov, and O. Kocharovskaya, Coherent control of the waveforms of recoilless γ-photons, Nature (London) **508**, 80 (2014).

[14] A. Santillán and S. I. Bozhevolnyi, Acoustic transparency and slow sound using detuned acoustic resonators, Phys. Rev. B **84**, 064304 (2011).

[15] M. Amin, A. Elayouch, M. Farhat, M. Addouche, A. Khelif, and H. Bağcı, Acoustically induced transparency using Fano resonant periodic arrays, J. Appl. Phys. **118**, 164901 (2015).

[16] V. Potapkin, A. I. Chumakov, G. V. Smirnov, J.-Ph. Celse, R. Ruffer, C. McCammon, and L. Dubrovinsky, A ^{57}Fe synchrotron Mössbauer source at the ESRF, J. Synchrotron Radiat. **19**, 559 (2012).

[17] T. Mitsui, R. Masuda, M. Seto, and N. Hirao, Variable-bandwidth ^{57}Fe synchrotron Mössbauer source, J. Phys. Soc. Jpn. **87**, 093001 (2018).

[18] F. Döring, A. L. Robisch, C. Eberl, M. Osterhoff, A. Ruhlandt, T. Liese, F. Schlenkrich, S. Hoffmann, M. Bartels, T. Salditt, and H. U. Krebs, Sub-5 nm hard X-ray point focusing by a combined Kirkpatrick Baez mirror and multilayer zone plate, Opt. Express **21**, 19311 (2013).

[19] E. Ikonen, P. Helistö, T. Katila, and K. Riski, Coherent transient effects due to phase modulation of recoilless γ radiation, Phys. Rev. A **32**, 2298 (1985).

[20] X. Zhang, W.-T. Liao, A. Kalachev, R. N. Shakhmuratov, M. O. Scully, and O. Kocharovskaya, Nuclear Quantum Memory and Time Sequencing of a Single γ Photon, Phys. Rev. Lett. **123**, 250504 (2019).

[21] E. Ikonen, P. Helistö, J. Hietaniemi, and T. Katila, Magnetic Phase Modulation of Recoilless Gamma Radiation by Nuclear Zeeman Effect, Phys. Rev. Lett. **60**, 643 (1988).

[22] Yu. V. Shvyd'ko, T. Hertrich, U. van Bürck, E. Gerdau, O. Leupold, J. Metge, H. D. Rüter, S. Schwendy, G. V. Smirnov, W. Potzel, and P. Schindelmann, Storage of Nuclear Excitation Energy Through Magnetic Switching, Phys. Rev. Lett. **77**, 3232 (1996).

[23] L. T. Tsankov, Experimental observations on the resonant amplitude modulation of Mössbauer gamma rays, J. Phys. A **14**, 275 (1981).

[24] Yu. V. Shvyd'ko and G. V. Smirnov, Enhanced yield into the radiative channel in Raman nuclear resonant forward scattering, J. Phys. Condens. Matter **4**, 2663 (1992).

[25] Y. V. Radeonychev, M. D. Tokman, A. G. Litvak, and O. Kocharovskaya, Acoustically Induced Transparency in Optically Dense Resonance Medium, Phys. Rev. Lett. **96**, 093602 (2006).

[26] R. N. Shakhmuratov, F. G. Vagizov, V. A. Antonov, Y. V. Radeonychev, M. O. Scully, and O. Kocharovskaya, Transformation of a single-photon field into bunches of pulses, Phys. Rev. A **92**, 023836 (2015).

[27] R. N. Shakhmuratov and F. G. Vagizov, Application of the Mössbauer effect to the study of subnanometer harmonic displacements in thin solids, Phys. Rev. B **95**, 245429 (2017).

[28] C. L. Chien and J. C. Walker, Mössbauer sidebands from a single parent line, Phys. Rev. B **13**, 1876 (1976).

[29] A. R. Mkrtchyan, G. A. Arutyunyan, A. R. Arakelyan, and R. G. Gabrielyan, Modulation of Mossbauer radiation by coherent ultrasonic excitation in crystals, Phys. Status Solidi (b) **92**, 23 (1979).

[30] E. K. Sadykov, A. A. Yurichuk, F. G. Vagizov, Sh. I. Mubarakshin, and A. A. Valiullin, Mössbauer spectroscopy under acoustical excitation: Thick target effects, Hyperfine Interact. **238**, 85 (2017).

[31] I. R. Khairulin, V. A. Antonov, Y. V. Radeonychev, and O. Kocharovskaya, Ultimate capabilities for compression of the waveform of a recoilless γ-ray photon into a pulse sequence in an optically deep vibrating resonant absorber, Phys. Rev. A **98**, 043860 (2018).

[32] I. R. Khairulin, V. A. Antonov, Y. V. Radeonychev, and O. Kocharovskaya, Transformation of Mössbauer γ-ray photon waveform into short pulses in dual-tone vibrating resonant absorber, J. Phys. B **51**, 235601 (2018).

[33] Y. V. Radeonychev, A. Polovinkin, and O. Kocharovskaya, Extremely Short Pulses via Stark Modulation of the Atomic Transition Frequencies, Phys. Rev. Lett. **105**, 183902 (2010).

[34] V. A. Antonov, T. R. Akhmedzhanov, Y. V. Radeonychev, and O. Kocharovskaya, Attosecond pulse formation via switching of resonant interaction by tunnel ionization, Phys. Rev. A **91**, 023830 (2015).

[35] V. A. Antonov, Y. V. Radeonychev, and O. Kocharovskaya, Formation of a Single Attosecond Pulse via Interaction of Resonant Radiation with a Strongly Perturbed Atomic Transition, Phys. Rev. Lett. **110**, 213903 (2013).

[36] See Supplemental Material at http://link.aps.org/supplemental/10.1103/PhysRevLett.124.163602 for more detailed description.

[37] E. Kuznetsova, O. Kocharovskaya, P. Hemmer, and M. O. Scully, Atomic interference phenomena in solids with a long-lived spin coherence, Phys. Rev. A **66**, 063802 (2002).

[38] V. Antonov, I. Khairulin, Y. Radeonychev, and O. Kocharovskaya, Modulation induced transparency of a Mössbauer resonant absorber, in *Proceedings of VII International Conference "Frontiers of Nonlinear Physics", Nizhny Novgorod, Russia, 2019* (Institute of Applied Physics, Russian Academy of Sciences, Nizhny Novgorod, 2019), pp. 222–223.

[39] I. R. Khairulin, V. A. Antonov, Y. V. Radeonychev, and O. Kocharovskaya, Acoustically induced transparency for synchrotron hard x-ray photons (to be published).

[40] B. P. Sorokin, G. M. Kvashnin, A. P. Volkov, V. S. Bormashov, V. V. Aksenenkov, M. S. Kuznetsov, G. I. Gordeev, and A. V. Telichko, AlN/single crystalline diamond piezoelectric structure as a high overtone bulk acoustic resonator, Appl. Phys. Lett. **102**, 113507 (2013).

[41] A. Ambrosy and K. Holdik, Piezoelectric PVDF films as ultrasonic transducers, J. Phys. E **17**, 856 (1984).

[42] R. N. Shakhmuratov, F. G. Vagizov, J. Odeurs, M. O. Scully, and O. Kocharovskaya, Slow γ photon with a doublet structure: Time delay via a transition from destructive to constructive interference of collectively scattered radiation with the incoming photon, Phys. Rev. A **80**, 063805 (2009).

[43] K. P. Heeg, J. Haber, D. Schumacher, L. Bocklage, H.-C. Wille, K. S. Schulze, R. Loetzsch, I. Uschmann, G. G. Paulus, R. Rüffer, R. Röhlsberger, and J. Evers, Tunable Subluminal Propagation of Narrow-band X-Ray Pulses, Phys. Rev. Lett. **114**, 203601 (2015).

[44] I. R. Khairulin, Y. V. Radeonychev, V. A. Antonov, and O. Kocharovskaya, Slowing gamma-ray photon in optically dense vibrating Mössbauer absorber, in *Proceedings of VII International Conference "Frontiers of Nonlinear Physics", Nizhny Novgorod, Russia, 2019* (Institute of Applied Physics, Russian Academy of Sciences, Nizhny Novgorod, 2019), pp. 234–235.

[45] I. R. Khairulin, Y. V. Radeonychev, and O. Kocharovskaya, Slow gamma-ray photons in vibrating optically deep recoilless absorber (to be published).